ARTICLE
Journal of Cellular Biochemistry 113:473–485 (2012)

Journal of Cellular Biochemistry

Isorhamnetin Inhibits H_2O_2-Induced Activation of the Intrinsic Apoptotic Pathway in H9c2 Cardiomyocytes Through Scavenging Reactive Oxygen Species and ERK Inactivation

Bing Sun, Gui-Bo Sun, Jing Xiao, Rong-Chang Chen, Xin Wang, Ying Wu, Li Cao, Zhi-Hong Yang, and Xiao-Bo Sun*

Research Center for Pharmacology and Toxicology, Institute of Medicinal Plant Development (IMPLAD), Chinese Academy of Medical Sciences & Peking Union Medical College, Beijing 100193, P. R. China

ABSTRACT

As a traditional Chinese medicine, the sea buckthorn (*Hippophae rhamnoides* L.) has a long history in the treatment of ischemic heart disease and circulatory disorders. However, the active compounds responsible for and the underlying mechanisms of these effects are not fully understood. In this article, isorhamnetin pretreatment counteracted H_2O_2-induced apoptotic damage in H9c2 cardiomyocytes. Isorhamnetin did not inhibit the death receptor-dependent or extrinsic apoptotic pathways, as characterized by its absence in both caspase-8 inactivation and tBid downregulation along with unchanged Fas and TNFR1 mRNA levels. Instead, isorhamnetin specifically suppressed the mitochondria-dependent or intrinsic apoptotic pathways, as characterized by inactivation of caspase-9 and -3, maintenance of the mitochondrial membrane potential ($\Delta\Psi$m), and regulation of a series of Bcl-2 family genes upstream of $\Delta\Psi$m. The anti-apoptotic effects of isorhamnetin were linked to decreased ROS generation. H_2O_2 activated ERK and p53, whereas isorhamnetin inhibited their activation. ERK overexpression overrode the isorhamnetin-induced inhibition of the intrinsic apoptotic pathway in H9c2 cardiomyocytes, which indicated that an ERK-dependent pathway was involved. Furthermore, *N*-acetyl cysteine (a potent ROS scavenger) could attenuate the H_2O_2-induced apoptosis. However, PD98059 (an ERK-specific inhibitor) could not effectively antagonize ROS generation, which indicates that ROS may be an upstream inducer of ERK. In conclusion, isorhamnetin inhibits the H_2O_2-induced activation of the intrinsic apoptotic pathway via ROS scavenging and ERK inactivation. Therefore, isorhamnetin is a promising reagent for the treatment of ROS-induced cardiomyopathy. J. Cell. Biochem. 113: 473–485, 2012.

KEY WORDS: ISORHAMNETIN; FLAVONOL; MYOCARDIAL APOPTOSIS; REACTIVE OXYGEN SPECIES; EXTRACELLULAR SIGNAL-REGULATED KINASE

Apoptosis plays a central role in cardiac remodeling, particularly in the transition toward overt heart failure because of the limited regenerative capacity of cardiomyocytes [Regula and Kirshenbaum, 2005]. Myocardial apoptosis during myocardial ischemia or clinical cardiac bypass surgery is frequently associated with the production and release of reactive oxygen species (ROS) [Davies et al., 1990; Krukenkamp et al., 1994]. ROS, which acts as a crucial inducer of ischemia and reperfusion injury, elicits an array of apoptotic damage, including membrane lipid peroxidation, cross-linking and degradation of proteins, nicking of DNA, and oxidative mitochondrial damage [von Harsdorf et al., 1999]. Additionally, studies have suggested that ROS is implicated in myocardial apoptosis as demonstrated by the induction of cardiomyopathies and early lethality in knockout mice that lack

Abbreviations used: Apaf-1, apoptotic protease activating factor-1; CAT, catalase; ERK, extracellular signal-regulated kinase; FADD, Fas-associated death domain; HE, hematoxylin and eosin; JC-1, 5,5′,6,6′-tetrachloro-1,1′,3,3′-tetraethylbenzimi-dazolylcarbocyanine iodide; JNK, c-Jun N-terminal protein kinase; LDH, lactate dehydrogenase; MAPKs, mitogen-activated protein kinases; $\Delta\Psi$m, mitochondrial membrane potential; NAC, *N*-acetylcysteine; PARP, poly(ADP-ribose) polymerase; PI, propidium iodide; PS, phosphatidyl serine; Real-time RT-PCR, real-time polymerase chain reaction; ROS, reactive oxygen species; SOD, superoxide dismutase; tBid, truncated Bid; TNFR1, tumor necrosis factor receptor-1; TUNEL, TdT-mediated dUTP-biotin nick end-labeling.

Grant sponsor: Major Scientific and Technological Special Project for "Significant New Drugs Formulation"; Grant number: 2009ZX09301-003.

*Correspondence to: Xiao-Bo Sun, Institute of Medicinal Plant Development (IMPLAD), Chinese Academy of Medical Sciences & Peking Union Medical College, No. 151, Malianwa North Road, Haidian District, Beijing 100193, P. R. China. E-mail: suntougao@gmail.com

Received 9 September 2011; Accepted 12 September 2011 • DOI 10.1002/jcb.23371 • © 2011 Wiley Periodicals, Inc.
Published online 21 September 2011 in Wiley Online Library (wileyonlinelibrary.com).

specific intracellular antioxidative enzymes, such as superoxide dismutase (SOD) [Li et al., 1995].

Two distinct pathways lead to myocardial apoptosis the mitochondria-dependent or intrinsic apoptotic pathway and the death receptor-dependent or extrinsic apoptotic pathway [Circu and Aw, 2010]. The intrinsic apoptotic pathway begins when an injury occurs within the cell. p53 is a sensor of cellular stress and initiates intrinsic apoptosis by transcriptionally regulating a series of Bcl-2 family genes. Moreover, p53 transactivates genes that lead to increased ROS and generalized oxidative damage to all mitochondrial components, which disrupts mitochondrial oxidative phosphorylation, thereby contributing to a number of human diseases, including ischemia/reperfusion injury [von Harsdorf et al., 1999; Circu and Aw, 2010]. The extrinsic apoptotic pathway begins outside a cell when conditions in the extracellular environment determine that a cell must die. Death receptors are cell surface receptors that transmit apoptotic signals initiated by specific ligands and play a central role in instructive apoptosis [Circu and Aw, 2010]. These receptors activate death caspases, such as caspase-8, causing apoptosis. The best-characterized death receptors are Fas and tumor necrosis factor receptor-1 (TNFR1). In both pathways, the activation of caspases, a family of cysteine proteases, leads to a proteolytic cascade to dismantle and remove the dying cell [Degterev et al., 2003].

Mitogen-activated protein kinases (MAPKs) are implicated in essential cellular events with regard to both cellular growth and apoptosis [Boulton et al., 1991; Su and Karin, 1996]. MAPKs are generally subdivided into three subgroups: p42/p44 extracellular signal-related kinases (ERK1/2), p38 MAPK, and c-Jun N-terminal protein kinase (JNK) [Boulton et al., 1991; Kyriakis et al., 1994], which have been demonstrated to function in distinct signaling pathways [Han et al., 1994; Whitmarsh and Davis, 1996]. MAPKs are activated in response to oxidant-induced alterations such as ROS generation [Fialkow et al., 1994; Ward et al., 1995]. Intracellular ROS reportedly induces distinct MAPK activation through inhibition of tyrosine phosphatases [Lee and Esselman, 2002; Zhou et al., 2002]. When activated, MAPKs lead to the phosphorylation of a host of different substrate proteins, including key regulatory enzymes, apoptosis regulators, and cytoskeletal proteins, by affecting the phosphorylation state of the substrate proteins [Zhou et al., 2002].

As a traditional Chinese medicine, the sea buckthorn (*Hippophae rhamnoides* L.) has a long history in the treatment of circulatory ischemic heart disease, disorders, liver damage, and cancer [Guliyev et al., 2004; Chawla et al., 2007]. In Tibetan medicine, the sea buckthorn is reputed as a panacea, and most prospective studies have indicated an inverse association between sea buckthorn flavonoid intake and heart disease [Suomela et al., 2006]. However, the active compounds responsible for and the underlying mechanisms of these cardioprotective effects are not fully understood. Isorhamnetin, the most abundant flavonol in the sea buckthorn, possesses many biological properties, including scavenging free radicals, increasing the resistance of low-density lipoprotein to oxidation and antitumor activity [Kong et al., 2009; Zhang et al., 2009; Kim et al., 2011]. Based on these findings, we hypothesized that isorhamnetin may exert protective effects against ROS-induced cardiomyopathy.

In the present study, we found that isorhamnetin pretreatment reduced H_2O_2-induced apoptosis in H9c2 cardiomyocytes. The data indicate that isorhamnetin may specifically reduce the activation of the intrinsic apoptotic pathway, as assessed by the expression of a host of apoptosis-related genes and caspase activities. The anti-apoptotic activity of isorhamnetin was also correlated with its ROS-scavenging effects and inactivation the ERK pathway.

MATERIALS AND METHODS

MATERIALS

Isorhamnetin was purchased from Shanghai Winherb Medical S & T Development (Shanghai, China). All tissue culture materials were from GIBCO (Grand Island, NY). JC-1 was purchased from Molecular Probes (Eugene, OR). All other antibodies were purchased from Santa Cruz Biotechnology (Santa Cruz, CA), and other chemicals were purchased from Sigma (St. Louis, MO) (Fig. 1).

CELL CULTURE AND TREATMENT

H9c2 cardiomyocytes were obtained from the Cell Bank of the Chinese Academy of Sciences (Shanghai, China) and cultured as previously described [Liu et al., 2008]. Briefly, H9c2 cardiomyocytes were maintained in Dulbecco's modified Eagle's medium with 4.5 g/L glucose supplemented with 10% (v/v) fetal bovine serum (FBS) and 1% penicillin/streptomycin (v/v) at 37°C in a humidified atmosphere containing 5% CO_2. H9c2 cardiomyocytes were treated with vehicle (0.1% DMSO) or isorhamnetin (from 0 to 50 μM) in the presence or absence of 150 μM H_2O_2 (4 h after) for various time periods, as indicated (2 or 6 h). For the ERK overexpression assay, H9c2 cardiomyocytes were transfected with either the wild-type ERK expression vector or an empty vector using Lipofectamine 2000 (Invitrogen, Carlsbad, CA). After 4 h of pretreatment with or without isorhamnetin (25 μM), the cells were exposed to H_2O_2 for 6 h. The cells were harvested at 4°C for further molecular and biochemical analyses.

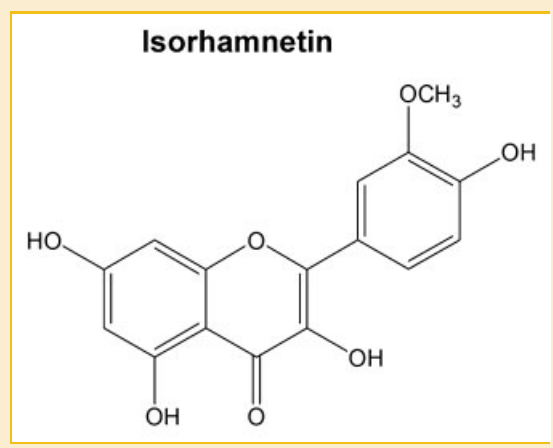

Fig. 1. Molecular structure of isorhamnetin.

ASSESSMENT OF CELL VIABILITY AND APOPTOSIS

Cell viability was determined using a 3-(4,5-dimethylthiazol-2-yl)-2,5-diphenyl tetrazolium bromide (MTT) assay as reported elsewhere [Xiao et al., 2010b]. Cell apoptosis was determined using terminal deoxynucleotidyl transferase-mediated dUTP nick end-labelling (TUNEL) assay with an in situ cell death detection kit and fluorescein (Roche Applied Science, Quebec, Canada) as previously described [Liu et al., 2008].

ASSESSMENT OF LDH RELEASE AND SOD AND CAT ACTIVITY

Lactate dehydrogenase (LDH) release was determined using a colorimetric cytotoxicity assay kit (CytoTox 96 Nonradioactive Cytotoxicity Assay; Promega, USA) as previously described [Xiao et al., 2010b]. SOD and CAT activity was measured using a detection kit according to the manufacturer's instructions.

DETECTION OF INTRACELLULAR ROS PRODUCTION

The level of intracellular ROS was determined using the total ROS detection kit (Enzo, USA) according to the manufacturer's protocol. Quantitative analysis of intracellular ROS production was determined using flow cytometry. For each analysis 10,000 events were recorded.

WESTERN BLOT ANALYSIS

Cell lysate preparation and Western blot analysis were performed as previously described [Xiao et al., 2010a]. The protein concentration was determined using the Bio-Rad DC Protein Determination Kit, with bovine serum albumin (BSA) as the standard. The immunoblots were developed using the ECL kit.

CASPASE-3, -8, AND -9 ACTIVITY ASSAY

Caspase-3, -8, and -9 activities were measured using the Fluorometric Assay Kit (BioVision, USA) according to the manufacturer's instructions. The samples were read in a Fluoroskan Ascent FL fluorometer (Thermo Fisher Scientific, USA) using 400-nm excitation and 505-nm emission wavelengths, and the results were expressed as fold change over the control.

MEASUREMENT OF MITOCHONDRIAL MEMBRANE POTENTIAL ($\Delta\Psi m$) USING JC-1

After each treatment, the cells grown on coverslips were incubated with 5 mM JC-1 dye (Molecular Probes) for 15 min at 37°C. The cells were washed with PBS and immediately analyzed using a confocal microscope. JC-1 fluorescence was measured from a single excitation wavelength (488 nm) with dual emission (a shift from green at 530 nm to red at 590 nm).

REAL-TIME POLYMERASE CHAIN REACTION (RT-PCR)

Total RNA was extracted using TRIzol (Invitrogen). A total of 2 μg of total RNA was reverse transcribed using the SuperScript First-Strand Synthesis System (Invitrogen). The cDNA was synthesized from isolated RNA, and cycle time (C_t) values were obtained using real-time RT-PCR with the Power SYBR Green PCR Master Mix (Applied Biosystems, Foster City, CA), iQ5 Real-Time PCR Detection System and analysis software (Bio-Rad, USA) as previously described [Sun et al., 2010]. The primers were designed using the Applied Biosystems Primer Express Software (version 2.0), and the primer sequences are shown in Table I.

STATISTICAL ANALYSIS

The data are expressed as the mean ± SE. The significance of the differences between the means was assessed using the Student's *t*-test, and *P*-values <0.05 were considered significant. A one-way ANOVA test with Bonferroni corrections was used to determine significance for multiple comparisons. The calculations were performed using the SPSS (version 11.0) statistical software.

RESULTS

THE EFFECTS OF ISORHAMNETIN ON CELL VIABILITY, LDH RELEASE, AND ROS-SCAVENGING ENZYME ACTIVITIES

Exposure of H9c2 cardiomyocytes to H_2O_2 led to a decrease in cell viability, whereas pretreatment with 12, 25, and 50 μM isorhamnetin maintained cell viability at roughly 65%, 76%, and 78%, respectively (Fig. 2A). As shown in Figure 2B–D, pretreatment

TABLE I. Primers Used for Real-Time RT-PCRs

	Primer pairs (5′–3′)	
Target genes	Forward	Reverse
Fas	TCGTGAAACCGACAACAACTG	CACGGTTGACAGCAAAATGG
TNFR1	GGCCGCGTGCTTTGC	TTCTAGAGTCTCGCGGATGTTCT
p53	CCCACCGCCTGTAAGATTCTAT	AATGGGTCCTGGAGGATACAGA
Bcl-2	CTGGGATGCCTTTGTGGAACT	TGAGCAGCGTCTTCAGAGACA
Bcl-w	CATCAGCACTGGGTCGTAAGAG	CTTCTGCCTCAGCTTATAGCCTACA
Bcl-xl	TGGTGAGTCGGATTGCAAGTT	CCGCCGTTCTCCTGGAT
Bfl	TCTTCAGTATGTCCTGCAGGTACCT	CAGATTCTTTTCAACTTCCTTTTGTACA
Bcl-Rambo	AGATTAGGTCTGCGGGTCGAA	TGCAGTAGAAGGGACGAAGGA
Bak1	GCTGGGAATGCCTACGAACTC	ACACGGCCCCAGCTGAT
Mcl-1	GGGCAGGATTGTGACTCTTATTTC	AGTCCCGCTTCGTCCTTACA
Bax	TGGAGCTGCAGAGGATGATTG	AGCTGCCACCCGGAAGA
Map-1	GCCTTGGTTGGGCTCACA	CTCCAGACACCTCCTTTTGCA
Bid	TGACTGTGTAAAAGACACTGGAGTGA	TCCCACCACCTGGAAATAGG
Bik	AGGTATTTTCAGAAGCTTGATTGGA	AGGGTCCTGGTCAGGTGACA
Bad	ATGGAGGCGCTGGGACTAT	CCATCCCTTCATCTTCCTCAGT
GAPDH	AACGACCCCTTCATTGAC	TCCACGACATACTCAGCAC

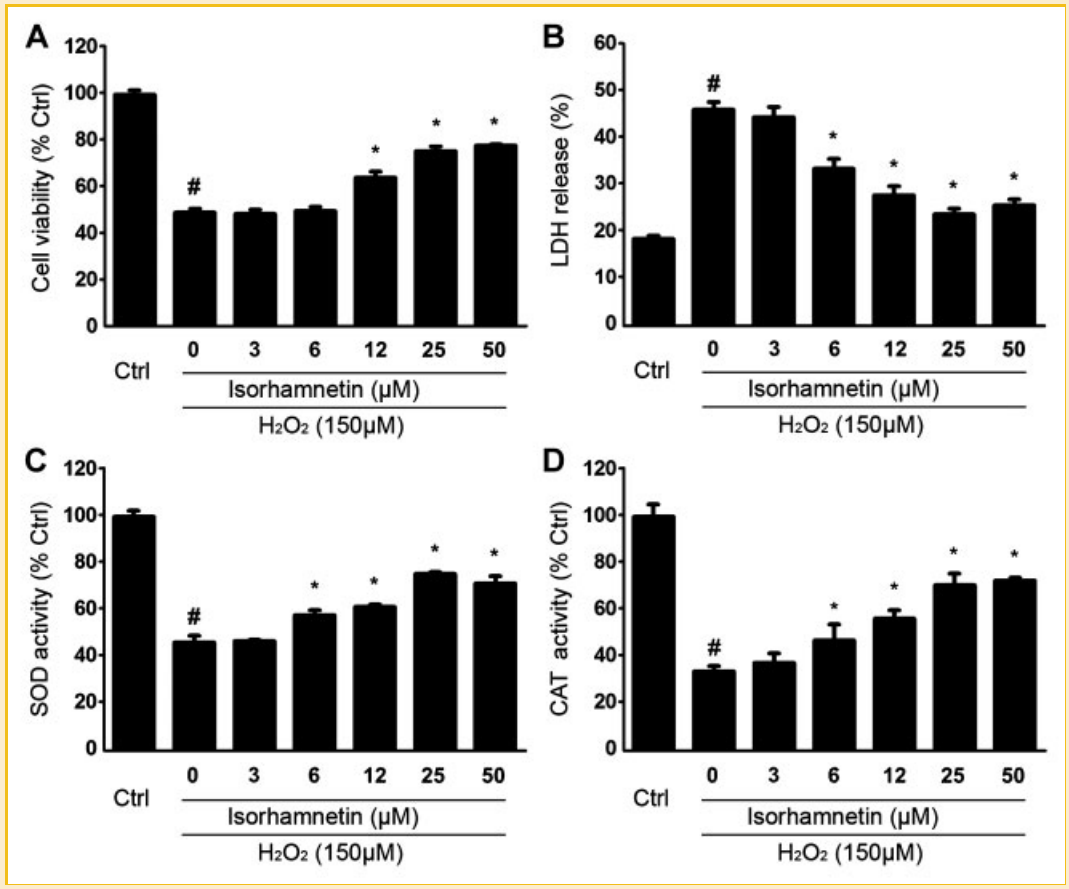

Fig. 2. The effects of H_2O_2 and isorhamnetin on cell viability, LDH release and the activities of SOD and CAT in H9c2 cardiomyocytes. H9c2 cardiomyocytes were treated with the vehicle or H_2O_2 (150 μM) for 6 h with isorhamnetin (0, 3, 6, 12, 25, 50 μM for 4 h prior to H_2O_2 exposure). Cell viability was determined using the MTT assay (A, expressed as the percentage of control). Isorhamnetin effects on LDH release were measured using the LDH activity assay (B, expressed as percent LDH). The activities of SOD and CAT were measured (C,D, expressed as the percentage of vehicle control). The results are represented as the mean ± SE (n = 8 per group). $^{\#}P < 0.05$ versus Ctrl; $^{*}P < 0.05$ versus H_2O_2-treated cells.

with 6, 12, and 25 μM isorhamnetin reduced H_2O_2-induced LDH release, while preserving the H_2O_2-induced loss of activity of SOD and CAT, two ROS-scavenging enzymes. Higher isorhamnetin concentrations (up to 50 μM) did not improve cell viability, LDH release, or the activity of ROS-scavenging enzymes. Therefore, 25 μM isorhamnetin was selected for subsequent experiments.

ISORHAMNETIN SUPPRESSES H_2O_2-INDUCED APOPTOSIS IN H9c2 CARDIOMYOCYTES

DNA fragmentation is the hallmark of apoptosis [Danial and Korsmeyer, 2004]; thus, we first evaluated the effect of isorhamnetin regarding this event. As shown in Figure 3A,B, the TUNEL assay revealed that H_2O_2 caused increased DNA fragmentation, which is in accordance with a previous study that showed that ROS induces apoptotic damage such as DNA fragmentation [von Harsdorf et al., 1999]. Isorhamnetin (25 μM) pretreatment attenuated H_2O_2-induced DNA fragmentation (Fig. 3A,B). Phosphatidyl serine (PS) exposure on the extracellular side of the cell membrane occurs during apoptosis [Yamaji-Hasegawa and Tsujimoto, 2006]. The Annexin-V/PI staining results revealed that isorhamnetin pretreatment inhibited H_2O_2-induced PS exposure, characterized by the decreased proportion of Annexin-V-stained cells (Fig. 3C,D). Furthermore, few PI-counterstained cells were seen in the present study, indicating that neither H_2O_2 nor isorhamnetin leads to cell necrosis. The immunoblotting assays indicated that isorhamnetin reduces cytochrome *c* release from the mitochondria into the cytosol without affecting the expression of prohibitin, a mitochondrial marker protein (Fig. 3E). In addition, two characterized apoptosis indicators, cleaved caspase-3 and cleaved poly(ADP-ribose) polymerase (PARP), were also inhibited by isorhamnetin pretreatment (Fig. 3E). However, isorhamnetin alone showed no obvious effects on these cleavage events (Fig. 3).

THE ANTI-APOPTOTIC EFFECTS OF ISORHAMNETIN ARE SPECIFICALLY RELATED TO THE INTRINSIC APOPTOTIC PATHWAY

Apoptosis is generally subdivided into two pathways, the intrinsic or mitochondria-dependent apoptotic pathway and the extrinsic or death receptor-dependent apoptotic pathway. As shown in Figure 4A, immunoblotting assays indicate that isorhamnetin pretreatment could not attenuate the H_2O_2-induced elevation in protein levels of tBid and cleaved caspase-8 but can inhibit caspase-9 cleavage. Caspase-8 is a well-known inducer of the death receptor-

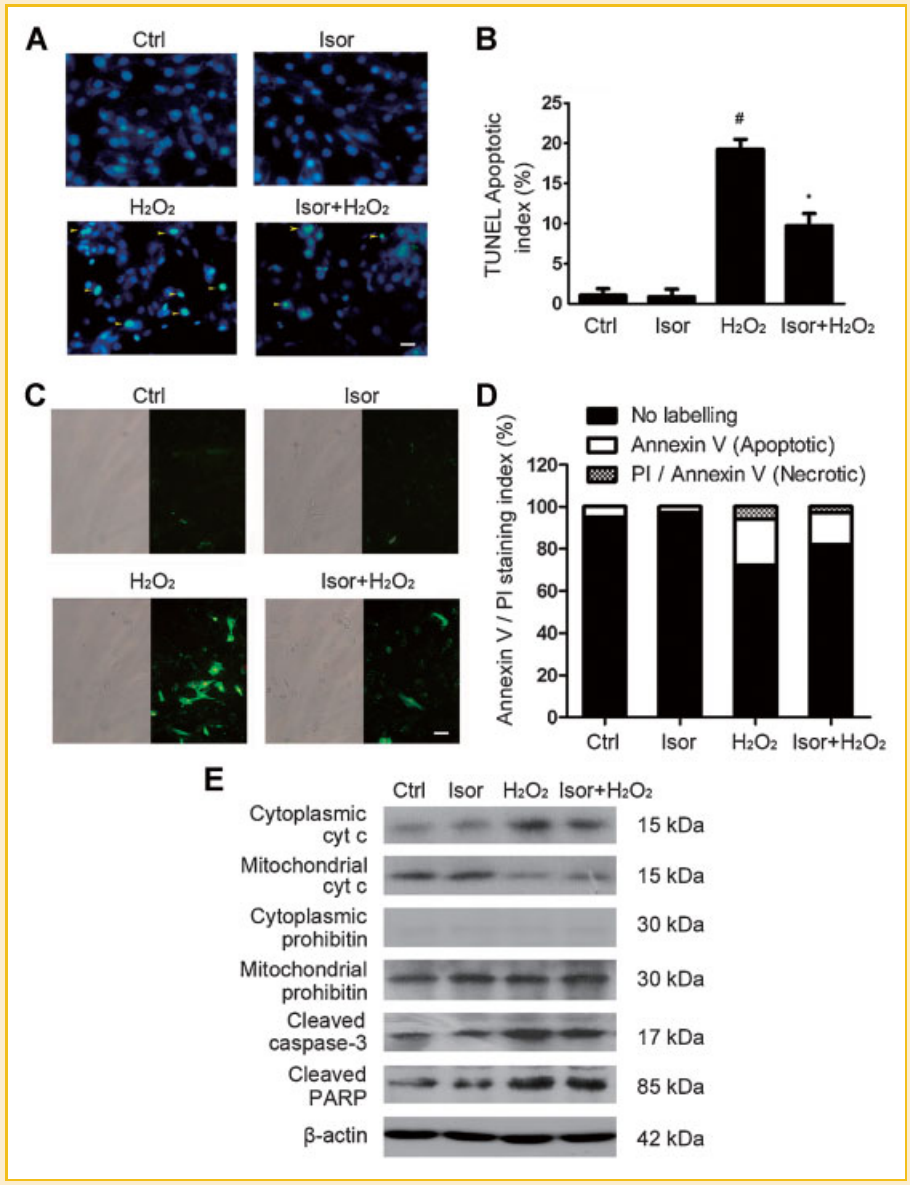

Fig. 3. The effects of H_2O_2 and isorhamnetin on apoptosis in H9c2 cardiomyocytes. After 4 h of pretreatment with or without isorhamnetin (25 μM), the cells were exposed to H_2O_2 and stained using the TUNEL assay (A). The arrowheads in the pictures indicate the nuclei of apoptotic cells; cell nuclei counterstained with DAPI are shown in blue (A, scale bar = 10 μm). The TUNEL apoptotic index was determined by calculating the ratio of TUNEL-positive cells to total cells (B). H9c2 cells were labeled with Annexin-V and PI (propidium iodide) (C, left panels: microscopic view of bright field; right panels: microscopic view of Annexin-V/PI staining; scale bar = 10 μm). The Annexin-V/PI staining index was determined by calculating the ratio of Annexin-V-positive or Annexin-V/PI-positive cells to total cells (D). Levels of cytochrome *c* (cyt *c*) and prohibitin in the mitochondrial and cytosolic protein extracts as well as cleaved caspase-3 and cleaved PARP were determined using Western blot analysis (E). The results are represented as the mean ± SE (n = 8 per group). $^{\#}P < 0.05$ versus Ctrl; $^{*}P < 0.05$ versus H_2O_2-treated cells. [Color figure can be seen in the online version of this article, available at http://wileyonlinelibrary.com/journal/jcb]

dependent pathway of apoptosis and, when activated, can lead to Bid cleavage into tBid (truncated Bid), subsequently triggering the execution phase of apoptosis [Regula and Kirshenbaum, 2005]. Isorhamnetin pretreatment also suppressed H_2O_2-induced activation of caspase-3 and -9 but had no obvious effects on caspase-8 (Fig. 4B). Our results suggest that isorhamnetin does not act through the extrinsic apoptotic pathway, which was further confirmed by the unchanged mRNA levels of Fas and TNFR1, the two best-characterized death receptors (Fig. 4C). However, p53, a stressor of the intrinsic apoptotic pathway, was downregulated by isorhamnetin pretreatment (Fig. 4C), which indicates that isorhamnetin may act specifically through the intrinsic apoptotic pathway.

Mitochondrial membrane potential ($\Delta\Psi m$) depolarization is closely related to activation of the intrinsic apoptotic pathway [Youle RJ and Strasser A, 2008]. Thus, we next assessed whether $\Delta\Psi m$ was disrupted by H_2O_2 but not by isorhamnetin. H9c2 cardiomyocytes were stained with the $\Delta\Psi m$ indicator JC-1, which emits red fluorescence in the mitochondria, with higher $\Delta\Psi m$ and green fluorescence in those losing $\Delta\Psi m$. As shown in Figure 4D,E, H_2O_2 caused less JC-1 red fluorescence in the H9c2 cardiomyocytes,

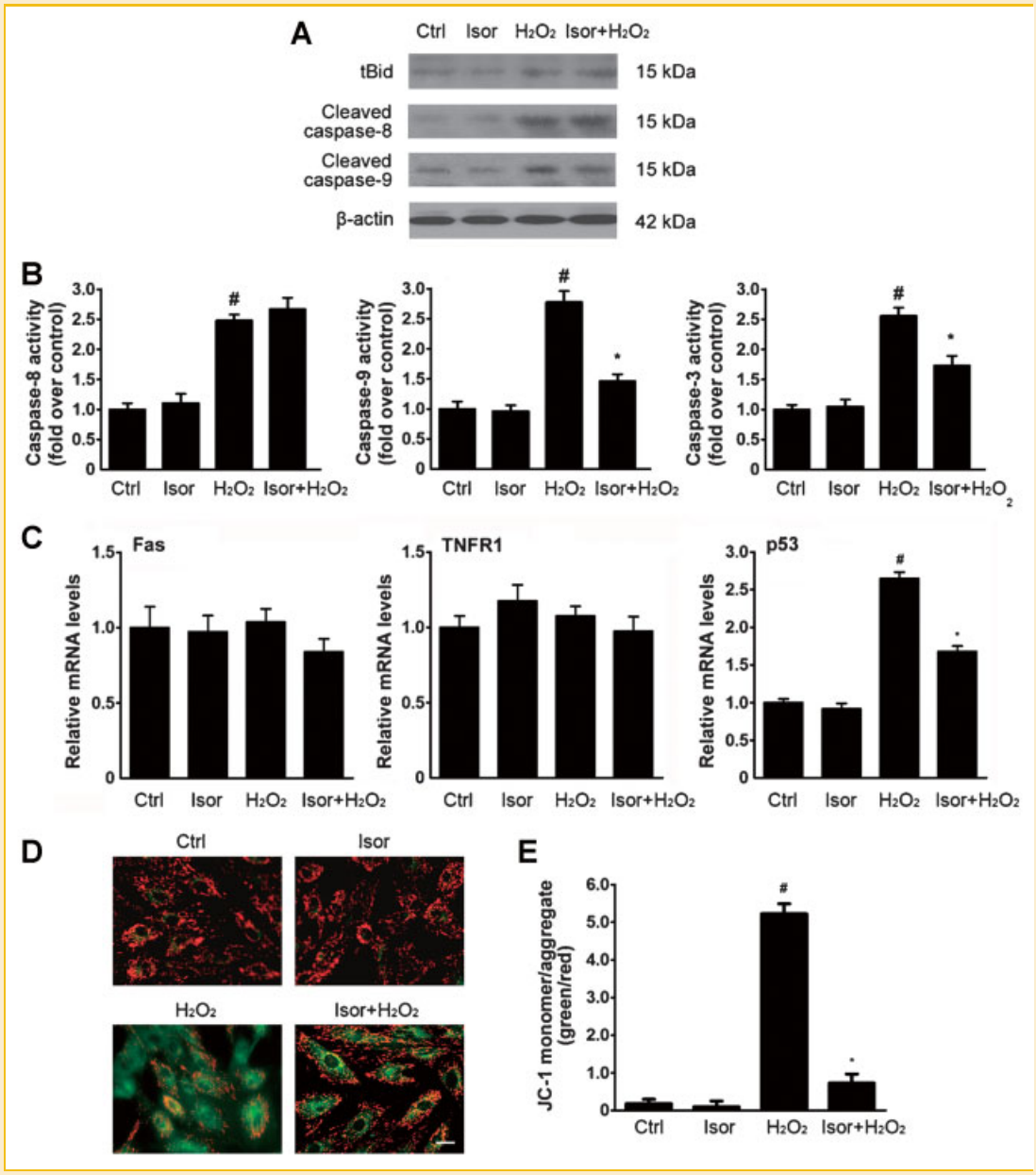

Fig. 4. Isorhamnetin specifically acts on the intrinsic apoptotic pathway. After 4 h of pretreatment with or without isorhamnetin (25 μM), the cells were exposed to H_2O_2. Levels of tBid, cleaved caspase-8 and cleaved caspase-9 were determined using Western blot analysis (A). The activities of caspase-8, -9, and -3 were measured using a fluorometric assay and expressed as the fold change over the control (B). The mRNA levels of Fas, TNFR1, and p53 were determined by real-time RT-PCR (C). The levels of mRNA were normalized to that of GAPDH. Relative mRNA levels are shown using arbitrary units, and the value of the control group is defined as 1. H9c2 cells were exposed to H_2O_2 and stained with JC-1 dye, which emits red fluorescence in mitochondria with a higher $\Delta\Psi m$ and green fluorescence in cells losing $\Delta\Psi m$. Representative pictures of JC-1 staining are shown (D, scale bar = 10 μm). Quantitative analysis of JC-1 staining was performed (E, green to red fluorescence ratio). The results are represented as the mean ± SE ($n = 8$ per group). $^{\#}P < 0.05$ versus Ctrl; $^{*}P < 0.05$ versus H_2O_2-treated cells. [Color figure can be seen in the online version of this article, available at http://wileyonlinelibrary.com/journal/jcb]

indicating perturbations in $\Delta\Psi m$, whereas pretreatment with isorhamnetin maintained $\Delta\Psi m$.

As is shown in Figure 4, isorhamnetin alone showed no obvious effects on these processes. Moreover, previous data have shown that isorhamnetin pretreatment inhibits cytochrome *c* release and cleavage of PARP and caspase-3 (Fig. 3E); therefore, isorhamnetin specifically acts on the intrinsic apoptotic pathway.

A SERIES OF Bcl-2 FAMILY GENES UPSTREAM OF $\Delta\Psi m$ IS TIGHTLY REGULATED BY ISORHAMNETIN

Because H_2O_2 caused $\Delta\Psi m$ depolarization and pretreatment with isorhamnetin maintained $\Delta\Psi m$ depolarization, we next investigated the mechanisms by which $\Delta\Psi m$ was maintained by isorhamnetin pretreatment. In the present study, we evaluated the mRNA levels of a series of Bcl-2 family genes upstream of $\Delta\Psi m$ regulation [Youle and Strasser, 2008], including the Bcl-2

anti-apoptotic genes as well as the Bax-like and BH3-only pro-apoptotic genes. As shown in Figure 5A, expression levels of the Bcl-2 anti-apoptotic genes Bcl-2, Bcl-xl, and Bfl-1 decreased after 6 h, but not after 2 h, of H_2O_2 exposure. Bcl-2 and Bfl-1 expression levels were preserved by isorhamnetin after 6 h of H_2O_2 exposure (Fig. 5A). Bcl-w expression levels did not significantly change after isorhamnetin treatment and H_2O_2 exposure. The Bax-like and the BH3-only pro-apoptotic-related genes increased after 2 and 6 h of H_2O_2 exposure (Fig. 5B,C). Isorhamnetin pretreatment preserved the expression of the Bax-like pro-apoptotic-related genes Bak1, Mcl-1, and Bax after 6 h of H_2O_2 exposure (Fig. 5B) as well as the expression of the BH3-only pro-apoptotic-related genes Map-1 and Bik after 2 h of H_2O_2 exposure (Fig. 5C). These results show that isorhamnetin upregulates Bcl-2-related genes and downregulates the BH3-only and Bax-like-related genes at different stages of H_2O_2 exposure.

ISORHAMNETIN REDUCES H_2O_2–INDUCED ROS GENERATION IN H9c2 CARDIOMYOCYTES

Several studies have suggested that flavonoids can induce variation in the level of cellular ROS [Areias et al., 2001; Hendriks et al., 2003]; therefore, we determined whether isorhamnetin shows a potent ROS-scavenging effect. Using a fluorescence assay (Fig. 6A) and quantitative flow cytometric approaches (Fig. 6B,C), we observed that H9c2 cardiomyocytes exposed to H_2O_2 displayed increased ROS production (approximately 43% vs. Ctrl), whereas pretreatment with 25 μM isorhamnetin reduced H_2O_2-induced ROS production. However, treatment with isorhamnetin alone did not induce any obvious ROS-scavenging effects compared to the control treatment. Thus, isorhamnetin may suppress apoptosis by directly scavenging ROS.

THE ERK SIGNALING PATHWAY IS INVOLVED IN THE ANTI-APOPTOTIC EFFECT OF ISORHAMNETIN

The MAPK signaling pathways are clearly involved in a host of cellular functions, including cell growth, differentiation, and apoptosis [Boulton et al., 1991; Han et al., 1994; Kyriakis et al., 1994; Lee et al., 1995; Su and Karin, 1996; Whitmarsh and Davis, 1996]. In general, MAPK signaling pathways are subdivided into three different pathways, namely the ERK, p38 kinase, and JNK signaling pathways [Boulton et al., 1991; Han et al., 1994; Kyriakis et al., 1994; Lee et al., 1995; Su and Karin, 1996]. Therefore, to determine whether the MAPK signaling pathway is involved in the anti-apoptotic effects of isorhamnetin, the cells were initially treated with kinase inhibitors, such as PD98059, SB202190, or SP600125, to ascertain which MAPK signaling pathway is involved in H_2O_2-induced apoptosis of H9c2 cardiomyocytes. Both SB202190 (a p38 kinase-specific inhibitor) and SP600125 (a JNK-specific inhibitor) were found to have little or no influence on the H_2O_2-induced loss of cell viability in H9c2 cardiomyocytes, whereas treatment with PD98059 (an ERK-specific inhibitor) was shown to suppress H_2O_2-induced cell death (Fig. 7A). Given that ERK1/2 and p53 were activated and have recently been reported to play crucial roles in the intrinsic apoptotic pathway [Liu et al., 2008], the effects of isorhamnetin on ERK1/2 and p53 activation were subsequently evaluated. As shown in Figure 7B, after 2 h of H_2O_2 exposure, ERK1/2 and p53 were phosphorylated and translocated into the nucleus, consistent with the findings of a previous study that showed that ERK1/2 phosphorylates p53, causing p53 cytoplasm-to-nucleus translocation and activation during the early stages of apoptosis [Liu et al., 2008]. However, isorhamnetin pretreatment led to the dephosphorylation of ERK1/2 and p53 along with decreased nuclear proportions of ERK1/2 and p53 after 2 and 6 h of H_2O_2 exposure (Fig. 7B,C). Pretreatment with PD98059 clearly antagonized H_2O_2-induced ERK and p53 phosphorylation, cleavage of PARP and caspase-3, $\Delta\Psi m$ depolarization, caspase-3 activation, and DNA fragmentation (Fig. 8). However, sustained ERK1/2 activation was observed in cells that had been exposed to H_2O_2 (Fig. 7B,C), indicating that sustained ERK activation may be involved in H_2O_2-induced apoptosis in H9c2 cardiomyocytes.

To confirm the involvement of ERK stimulation in the anti-apoptotic effects associated with isorhamnetin, H9c2 cardiomyocytes were transfected with wild-type ERK or empty plasmids. ERK overexpression was shown to significantly override the anti-apoptotic functions of isorhamnetin, but this was not observed in the cells transfected with the empty plasmid (Fig. 7D–G). When ERK was overexpressed, significant levels of recovery were registered with regard to both ERK and p53 phosphorylation and cleavage of PARP and caspase-3 (Fig. 7D). The JC-1-staining $\Delta\Psi m$ analysis also shows that ERK overexpression overrides the isorhamnetin-induced maintenance of $\Delta\Psi m$ (Fig. 7E). However, when ERK was overexpressed, no additional ROS production was detected (Fig. 7E). Furthermore, ERK overexpression exerted an antagonistic effect on the anti-apoptotic effects of isorhamnetin, including caspase-3 inactivation and DNA fragmentation (Fig. 7F,G). These data demonstrate that the ERK signaling pathway is intimately involved in the anti-apoptotic effects associated with isorhamnetin.

SUPPRESSION OF THE ROS-ERK SIGNALING PATHWAY PLAYS AN IMPORTANT ROLE IN APOPTOSIS REGULATION IN H9c2 CARDIOMYOCYTES

As shown in Figure 8A, the addition of *N*-acetyl cysteine (NAC), a well-known antioxidant and free radical scavenger, clearly antagonized the H_2O_2-induced phosphorylation of ERK and p53 as well as the concomitant cleavage of caspase-3 and PARP (Fig. 8A). The addition of NAC also suppressed both H_2O_2-induced apoptotic effects, including $\Delta\Psi m$ depolarization, caspase-3 activation, and DNA fragmentation (Fig. 8B–D). The ROS staining assay revealed that H_2O_2-induced ROS generation was wholly antagonized because of the addition of NAC (Fig. 8B). These data suggest that H_2O_2 induces both ERK activation and apoptosis in H9c2 cardiomyocytes via the generation of intracellular ROS. However, PD98059 (an ERK-specific inhibitor) could not effectively antagonize the H_2O_2-induced ROS generation (Fig. 8B). Moreover, in conjunction with previous data showing that ERK overexpression has little influence on ROS production (Fig. 7E), ROS may be an upstream regulator of ERK. Most importantly, the addition of isorhamnetin has an obvious inhibitory influence on the activation of ROS-ERK signaling pathways.

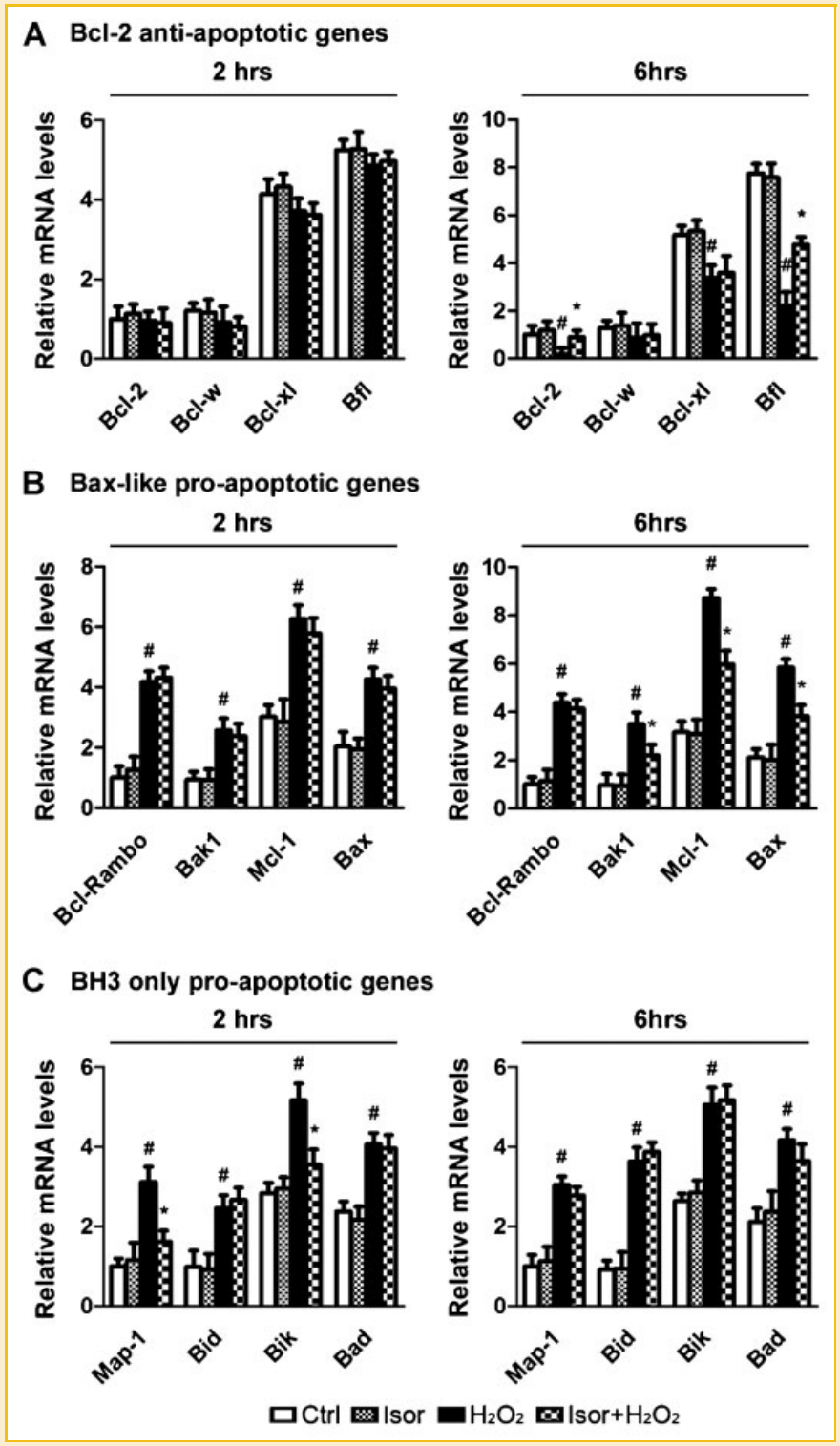

Fig. 5. The mRNA expression levels of a series of Bcl-2 family genes in different stages of apoptosis. After 4 h of pretreatment with or without isorhamnetin (25 μM), the cells were exposed to H_2O_2 for 2 or 6 h. The expression profiles of Bcl-2 anti-apoptotic (A), Bax-like (B), and BH3-only pro-apoptotic (C) genes in the early (2 h of H_2O_2 exposure) and late (6 h of H_2O_2 exposure) stages of apoptosis were determined by real-time RT-PCR. The levels of mRNA were normalized to that of GAPDH. Relative mRNA levels are shown using arbitrary units, and the value of Bcl-2 (A), Bcl-Rambo (B), or Map-1 (C) was defined as 1. The results are represented as the mean ± SE (n = 8 per group). $^{\#}P < 0.05$ versus Ctrl; $^{*}P < 0.05$ versus H_2O_2-treated cells.

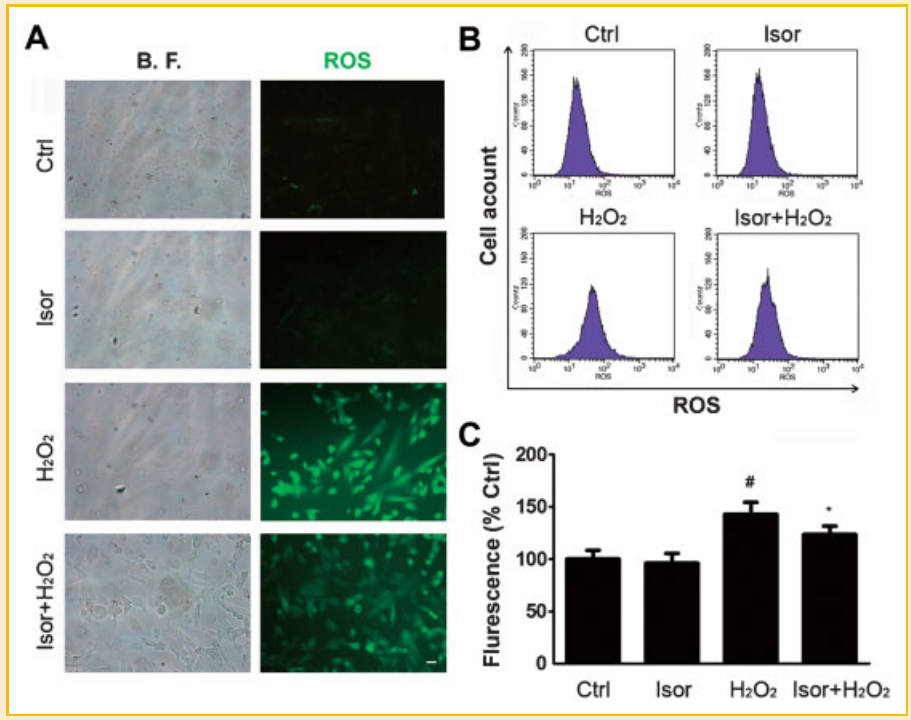

Fig. 6. The effects of H_2O_2 and isorhamnetin on intracellular ROS generation. After 4 h of pretreatment with or without isorhamnetin (25 μM), the cells were exposed to H_2O_2 for 6 h and assayed using a ROS detection kit (A, left: microscopic view of bright field; right: microscopic view of ROS staining; scale bar = 10 μm). Representative ROS staining histogram of H9c2 cells using flow cytometric analysis (B). Statistical analysis of ROS generation (C). The results are represented as the mean ± SE (n = 8 per group). $^{\#}P < 0.05$ versus Ctrl; $^{*}P < 0.05$ versus H_2O_2-treated cells. [Color figure can be seen in the online version of this article, available at http://wileyonlinelibrary.com/journal/jcb]

DISCUSSION

Isorhamnetin, the most abundant flavonol in sea buckthorn, is a potent ROS scavenger with complex functions in many pathological processes [Kong et al., 2009; Zhang et al., 2009; Kim et al., 2011]. In the current study, the protective effects of isorhamnetin against ROS-induced myocardial apoptosis and the underlying mechanisms were explored.

Evidence in the present study indicates that isorhamnetin pretreatment effectively antagonized H_2O_2-induced apoptotic damage, such as DNA fragmentation, PS exposure, $\Delta\Psi$m depolarization, cytochrome *c* release, and caspase-3 activation. Further studies suggest that isorhamnetin may specifically act through the intrinsic apoptotic pathway, as indicated by its absence in both caspase-8 inactivation and tBid downregulation along with the unchanged mRNA levels of Fas and TNFR1, the two best-characterized death receptors that initiate the extrinsic apoptotic pathway. The extrinsic (death receptor-initiated) pathway is initiated by the engagement of cell surface death receptors, which contain a cytoplasmic domain involved in protein–protein interactions and delivering apoptotic signals [Circu and Aw, 2010]. When Fas is cross-linked with its ligand, cytoplasmic death domains form a binding site for an adapter protein called Fas-associated death domain (FADD). Upon recruitment by FADD, pro-caspase8 oligomerization drives its activation through self-cleavage. Active caspase-8 then activates downstream caspase-3, committing the cell to apoptosis. Although isorhamnetin exhibits potent ROS-scavenging activities, isorhamnetin pretreatment does not effectively inhibit H_2O_2-induced caspase-8 activation. The data show that two of the well-known death receptors were also not upregulated by H_2O_2 exposure, which clearly indicates that caspase-8 is not activated by death receptors. Several studies have indicated that some factors other than death receptors can also lead to caspase-8 activation and are implicated in many pathologic processes [Krueger et al., 2001; Li et al., 2007; Borrelli et al., 2009]. When activated, caspase-8 cleaves Bid into tBid. The tBid translocates to the mitochondria where it triggers cytochrome *c* release from the mitochondrial intermembrane space. The released cytochrome *c* binds to apoptotic protease activating factor-1 (Apaf-1) together with procaspase-9 and activates caspase-9. The caspase-9 cleaves procaspase-3 and activates caspase-3. On the other hand, caspase-8 directly cleaves pro-caspase-3 [Jung and Kim, 2004]. In the present study, the isorhamnetin-induced caspase-3 inactivation was not caused by either caspase-8 or tBid but specifically through the activation of the intrinsic apoptotic pathway. Our findings also demonstrate that a series of Bcl-2 family proteins are tightly regulated by isorhamnetin, which may have a direct influence on mitochondrial membrane pore formation, the subsequent inhibition of cytochrome *c* release and its binding with both Apaf-1 and active caspase-9 result in caspase-3 inactivation, thereby leading to activation of the intrinsic apoptotic pathway. The regulation of Bcl-2 family genes may be directly transactivated by p53, a sensor of cellular stress that initiates intrinsic apoptosis by transcriptionally regulating a series of Bcl-2 family genes [Hemann and Lowe, 2006].

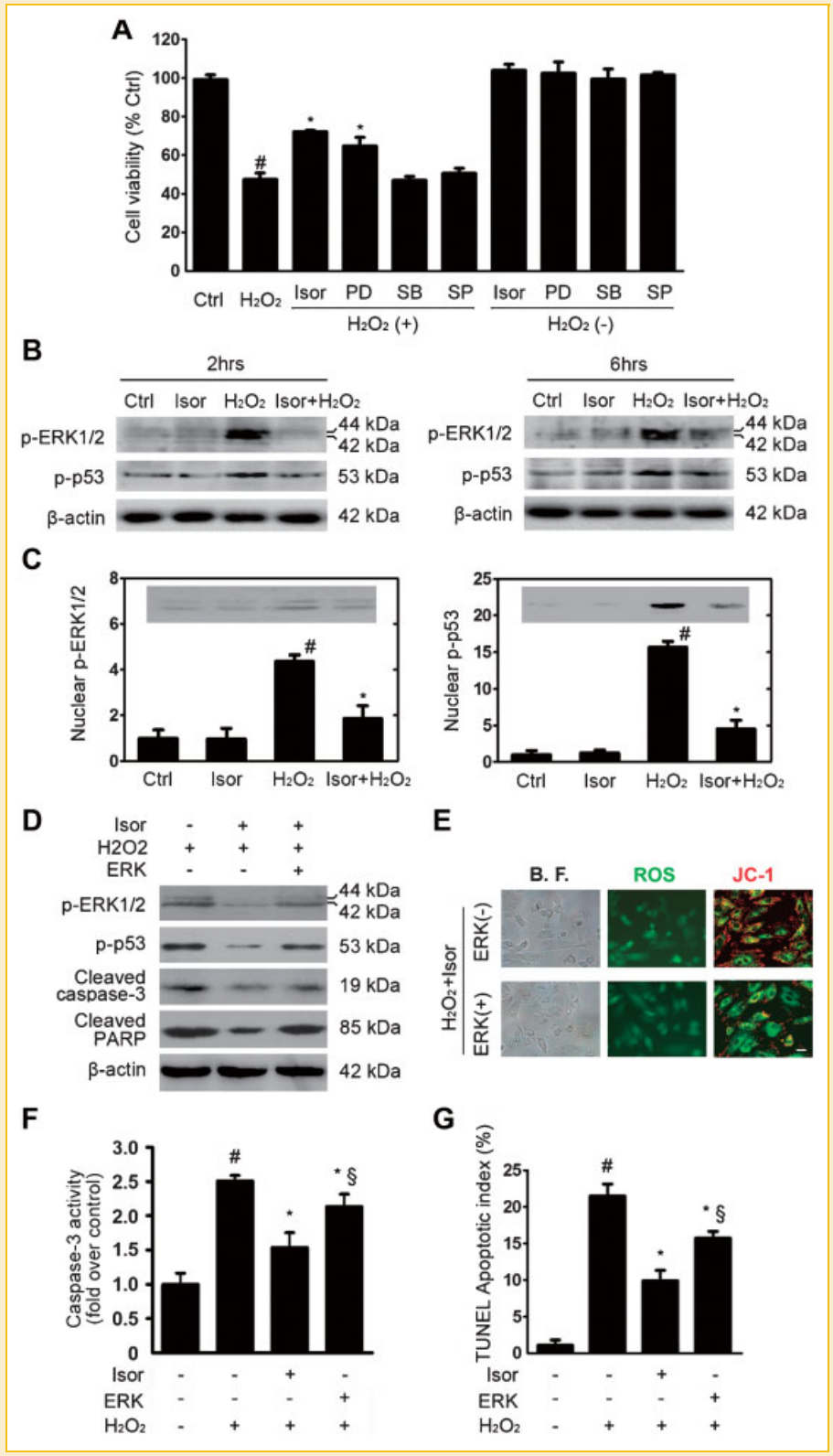

Fig. 7. The ERK signaling pathway is involved in the anti-apoptotic effects of isorhamnetin. After 4 h of pretreatment with or without isorhamnetin (25 μM), the cells were exposed to H_2O_2. The effects of the pharmacological inhibitors PD98059 (an ERK1/2-specific inhibitor), SB203580 (a p38-specific inhibitor), or SP600125 (a JNK-specific inhibitor) on cell viability were determined using the MTT assay (A). The protein levels of phospho-p53 (p-p53) and phospho-ERK1/2 (p-ERK1/2) were determined using Western blot analysis (B). The protein levels of p-ERK1/2 and p-p53 in the nuclear extracts were measured using Western blot analysis (C). H9c2 cells were transfected with the ERK expression vector or an empty vector. Transfected cells pretreated with or without isorhamnetin (25 μM) for 4 h were exposed to H_2O_2. The protein levels of phospho-p53 (p-p53), phospho-ERK1/2 (p-ERK1/2), cleaved caspase-3, and cleaved PARP were determined using Western blot analysis (D). The effects of ERK overexpression on ROS generation and $\Delta\Psi m$ were investigated (E, representative pictures from left to right are bright field, ROS staining and JC-1 staining; scale bar = 10 μm). The effects of ERK overexpression on caspase-3 activity (F) and the TUNEL apoptotic index (G) were investigated. The results are represented as the mean ± SE (n = 8 per group). $^{\#}P < 0.05$ versus Ctrl; $^{*}P < 0.05$ versus H_2O_2-treated cells; $^{\S}P < 0.05$ versus isorhamnetin pretreatment. [Color figure can be seen in the online version of this article, available at http://wileyonlinelibrary.com/journal/jcb]

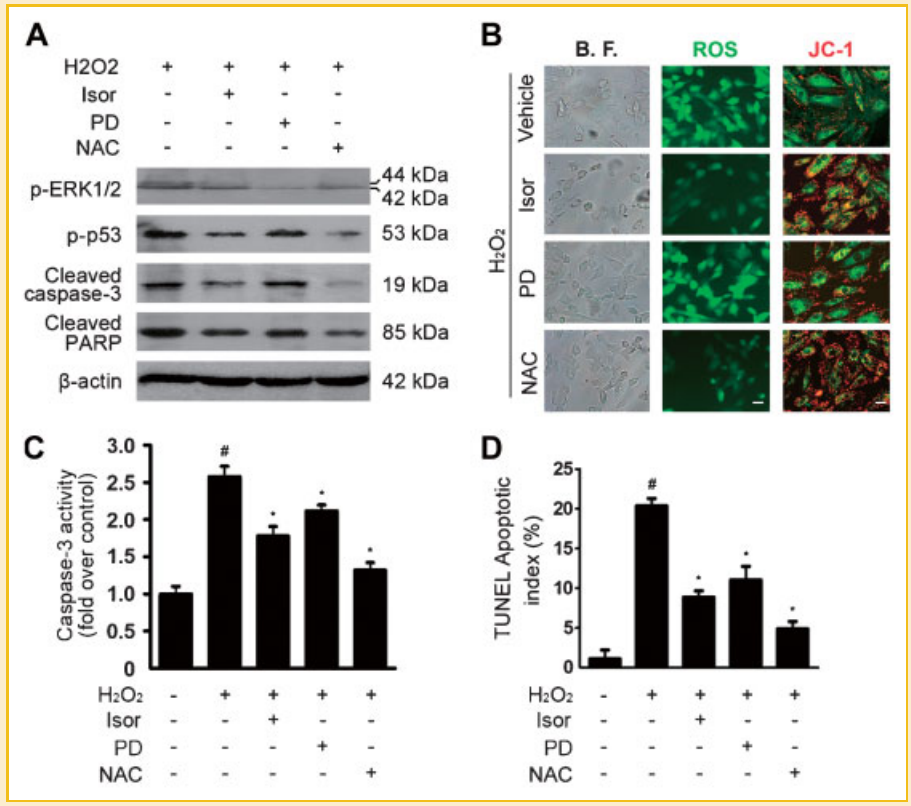

Fig. 8. ROS generation is upstream of ERK activation in isorhamnetin-induced apoptosis in H9c2 cardiomyocytes. The effects of NAC (a potent ROS scavenger) and PD98059 (an ERK1/2-specific inhibitor) on the protein levels of p-ERK1/2, p-p53, cleaved caspase-3, and cleaved PARP were determined using Western blot analysis (A). The effects of NAC and PD98059 on ROS generation and mitochondrial membrane potential ($\Delta\Psi m$) were investigated (B, representative pictures from left to right are bright field, ROS staining and JC-1 staining; scale bar = 10 μm). The effects of NAC and PD98059 on caspase-3 activity (C) and the TUNEL apoptotic index (D). The results are represented as the mean ± SE (n = 8 per group). $^{\#}P < 0.05$ versus Ctrl; $^{*}P < 0.05$ versus H_2O_2-treated cells. [Color figure can be seen in the online version of this article, available at http://wileyonlinelibrary.com/journal/jcb]

These findings are in accordance with our results, which show that both the mRNA and protein levels of p53 are upregulated by isorhamnetin pretreatment (Figs. 4C and 7B,C). Studies have also demonstrated that p53 can transactivate genes that lead to increased ROS, thereby augmenting oxidative damage [Haupt et al., 2003]. In contrast, isorhamnetin, with ROS-scavenging activity, may antagonize the oxidative damage.

Flavonoids are phenolic compounds that modulate apoptosis, differentiation, and the cell cycle, likely through their antioxidant functions [Fu et al., 2004]. In the present study, using H_2O_2 exposure to generate ROS, isorhamnetin pretreatment was observed to neutralize the reduction in cell viability, SOD and CAT activity, and increased LDH release and ROS production induced by H_2O_2 exposure (Figs. 2 and 6). These results directly reveal that the protective effects of isorhamnetin contribute to its role in ROS scavenging. To date, several studies have shown that some flavonoids, including 50 μM isorhamnetin, cause cytoxicity in some cancer cells via ROS generation [van Acker et al., 1997]. Controversies have also arisen regarding the possible antioxidant properties possessed by several flavonoids that reportedly function as either pro- or antioxidant compounds, depending on their concentration [Cemeli et al., 2004; Shen et al., 2004]. This may partially explain why isorhamnetin with a higher concentration (up to 50 μM) provided no additional benefits regarding cell viability or ROS-scavenging activities. The detailed molecular mechanisms for the decreased ROS-scavenging activity of isorhamnetin at higher concentrations need to be investigated further. Another issue that should be noted is that isorhamnetin reversed only 50% of H_2O_2 action. One reason for this might be that most of the H_2O_2-induced cellular damage on cellular proteins, lipids, and DNA was largely irreversible. It is well documented that a mere transient increase in mitochondrial membrane hyperpolarization after exposure to H_2O_2 initiates the collapse of $\Delta\Psi m$, mitochondrial translocation of Bax and Bad, and cytochrome *c* release [Circu and Aw, 2010]. Significant mitochondrial loss of cytochrome *c* leads to a further ROS increase due to a disrupted electron transport chain. The stress-induced sequential apoptotic signal cascade and ROS-induced ROS generation further exacerbate the damages induced by H_2O_2, and this may partially explain the limited reversal of the H_2O_2-induced effects by isorhamnetin.

The experiments demonstrated that sustained ERK activation is involved in the H_2O_2-induced apoptosis in H9c2 cardiomyocytes and that the anti-apoptotic effects associated with isorhamnetin are attributable to the suppression of H_2O_2-induced ERK activation. The addition of NAC, a well-known antioxidant, effectively suppresses both H_2O_2-induced ERK phosphorylation and apoptotic damage,

indicating that ERK activation can be attributed to intracellular ROS generation and is readily suppressed by isorhamnetin treatment (Fig. 8). ROS-dependent redox cycling is considered important in modulating key factors in signal transduction and carcinogenesis, particularly MAPKs and ERK [Lee and Esselman, 2002; Zhou et al., 2002]. However, whether ERK is activated during apoptosis remains unclear. Generally, the ERK cascade is believed to mediate both cell proliferation and survival [Cheng et al., 1998; Townsend et al., 1998; Rytomaa et al., 2000; Lenferink et al., 2001; Tran et al., 2001]. However, recent studies have demonstrated that the sustained activation of ERK is also involved in the apoptotic process [Zhou et al., 2002; Tantini et al., 2004; Plotkin et al., 2005]. Robust ERK stimulation reportedly suppresses the cell cycle via the expression of cell-cycle inhibitor proteins, including p21Cip/Waf and p27KIP [Marshall, 1999]. Moreover, ERK activation has been studied in terms of apoptosis mediation elicited by H_2O_2 or other oxidants in T cells, Jurkat T cells, and neutrophils [Lee and Esselman, 2002; Zhou et al., 2002]. In the present study, H_2O_2-induced cell death was inhibited by the addition of isorhamnetin and PD98059 (an ERK-specific inhibitor), whereas ERK overexpression significantly overrode the anti-apoptotic effects of isorhamnetin. However, neither ERK overexpression nor the ERK-specific inhibitor influenced ROS production (Figs. 7E and 8B), which suggests that ROS may be an upstream regulator of the ERK signaling pathway that contributes to apoptosis modulation by isorhamnetin in cardiomyocytes.

In summary, isorhamnetin protects against H_2O_2-induced myocardial apoptosis in H9c2 cardiomyocytes via its effects on inhibition of the mitochondria-dependent intrinsic apoptotic pathway, ROS scavenging, and mediation of the ERK signaling pathway. Although animal studies are needed, isorhamnetin is a promising agent for the treatment of ROS-induced heart injuries such as myocardial ischemia/reperfusion injuries and may have implications for other diseases associated with ROS, such as neurodegenerative disorders.

Highlights

(1) Isorhamnetin selectively inhibits the activation of intrinsic apoptotic pathway.
(2) Isorhamnetin pretreatment reduces the generation of reactive oxygen species (ROS).
(3) Isorhamnetin inhibits extracellular signal-regulated kinase (ERK) pathway.
(4) A series of Bcl-2 family genes is tightly regulated by isorhamnetin.

ACKNOWLEDGMENTS

This study was supported by Major Scientific and Technological Special Project for ''Significant New Drugs Formulation'' (2009ZX09301-003).

REFERENCES

Areias FM, Rego AC, Oliveira CR, Seabra RM. 2001. Antioxidant effect of flavonoids after ascorbate/Fe(2+)-induced oxidative stress in cultured retinal cells. Biochem Pharmacol 62:111–118.

Borrelli S, Candi E, Alotto D, Castagnoli C, Melino G, Vigano MA, Mantovani R. 2009. p63 regulates the caspase-8-FLIP apoptotic pathway in epidermis. Cell Death Differ 16:253–263.

Boulton TG, Nye SH, Robbins DJ, Ip NY, Radziejewska E, Morgenbesser SD, DePinho RA, Panayotatos N, Cobb MH, Yancopoulos GD. 1991. ERKs: A family of protein-serine/threonine kinases that are activated and tyrosine phosphorylated in response to insulin and NGF. Cell 65:663–675.

Cemeli E, Schmid TE, Anderson D. 2004. Modulation by flavonoids of DNA damage induced by estrogen-like compounds. Environ Mol Mutagen 44:420–426.

Chawla R, Arora R, Singh S, Sagar RK, Sharma RK, Kumar R, Sharma A, Gupta ML, Prasad J, Khan HA, Swaroop A, Sinha AK, Gupta AK, Tripathi RP, Ahuja PS. 2007. Radioprotective and antioxidant activity of fractionated extracts of berries of Hippophae rhamnoides. J Med Food 10:101–109.

Cheng M, Sexl V, Sherr CJ, Roussel MF. 1998. Assembly of cyclin D-dependent kinase and titration of p27Kip1 regulated by mitogen-activated protein kinase kinase (MEK1). Proc Natl Acad Sci USA 95:1091–1096.

Circu ML, Aw TY. 2010. Reactive oxygen species, cellular redox systems, and apoptosis. Free Radic Biol Med 48:749–762.

Danial NN, Korsmeyer SJ. 2004. Cell death: Critical control points. Cell 116:205–219.

Davies SW, Ranjadayalan K, Wickens DG, Dormandy TL, Timmis AD. 1990. Lipid peroxidation associated with successful thrombolysis. Lancet 335:741–743.

Degterev A, Boyce M, Yuan J. 2003. A decade of caspases. Oncogene 22:8543–8867.

Fialkow L, Chan CK, Rotin D, Grinstein S, Downey GP. 1994. Activation of the mitogen-activated protein kinase signaling pathway in neutrophils. Role of oxidants. J Biol Chem 269:31234–31242.

Fu Y, Hsieh TC, Guo J, Kunicki J, Lee MY, Darzynkiewicz Z, Wu JM. 2004. Licochalcone-A, a novel flavonoid isolated from licorice root (Glycyrrhiza glabra), causes G2 and late-G1 arrests in androgen-independent PC-3 prostate cancer cells. Biochem Biophys Res Commun 322:263–270.

Guliyev VB, Gul M, Yildirim A. 2004. Hippophae rhamnoides L.: Chromatographic methods to determine chemical composition, use in traditional medicine and pharmacological effects. J Chromatogr B Analyt Technol Biomed Life Sci 812:291–307.

Han J, Lee JD, Bibbs L, Ulevitch RJ. 1994. A MAP kinase targeted by endotoxin and hyperosmolarity in mammalian cells. Science 265:808–811.

Haupt S, Berger M, Goldberg Z, Haupt Y. 2003. Apoptosis—The p53 network. J Cell Sci 116:4077–4085.

Hemann MT, Lowe SW. 2006. The p53-Bcl-2 connection. Cell Death Differ 13:1256–1259.

Hendriks JJ, de Vries HE, van der Pol SM, van den Berg TK, van Tol EA, Dijkstra CD. 2003. Flavonoids inhibit myelin phagocytosis by macrophages; a structure-activity relationship study. Biochem Pharmacol 65:877–885.

Jung JY, Kim WJ. 2004. Involvement of mitochondrial- and Fas-mediated dual mechanism in CoCl2-induced apoptosis of rat PC12 cells. Neurosci Lett 371:85–90.

Kim JE, Lee DE, Lee KW, Son JE, Seo SK, Li J, Jung SK, Heo YS, Mottamal M, Bode AM, Dong Z, Lee HJ. 2011. Isorhamnetin suppresses skin cancer through direct inhibition of MEK1 and PI3-K. Cancer Prev Res (Phila) 4:582–591.

Kong CS, Kim JA, Qian ZJ, Kim YA, Lee JI, Kim SK, Nam TJ, Seo Y. 2009. Protective effect of isorhamnetin 3-O-beta-D-glucopyranoside from Salicornia herbacea against oxidation-induced cell damage. Food Chem Toxicol 47:1914–1920.

Krueger A, Schmitz I, Baumann S, Krammer PH, Kirchhoff S. 2001. Cellular FLICE-inhibitory protein splice variants inhibit different steps of caspase-8 activation at the CD95 death-inducing signaling complex. J Biol Chem 276:20633–20640.

Krukenkamp IB, Burns P, Caldarone C, Levitsky S. 1994. Perfusion and cardioplegia. Curr Opin Cardiol 9:247–253.

Kyriakis JM, Banerjee P, Nikolakaki E, Dai T, Rubie EA, Ahmad MF, Avruch J, Woodgett JR. 1994. The stress-activated protein kinase subfamily of c-Jun kinases. Nature 369:156–160.

Lee K, Esselman WJ. 2002. Inhibition of PTPs by H(2)O(2) regulates the activation of distinct MAPK pathways. Free Radic Biol Med 33:1121–1132.

Lee SH, Fujita N, Imai K, Tsuruo T. 1995. Cysteine produced from lymph node stromal cells suppresses apoptosis of mouse malignant T-lymphoma cells. Biochem Biophys Res Commun 213:837–844.

Lenferink AE, Busse D, Flanagan WM, Yakes FM, Arteaga CL. 2001. ErbB2/neu kinase modulates cellular p27(Kip1) and cyclin D1 through multiple signaling pathways. Cancer Res 61:6583–6591.

Li Y, Huang TT, Carlson EJ, Melov S, Ursell PC, Olson JL, Noble LJ, Yoshimura MP, Berger C, Chan PH, Wallace DC, Epstein CJ. 1995. Dilated cardiomyopathy and neonatal lethality in mutant mice lacking manganese superoxide dismutase. Nat Genet 11:376–381.

Li W, Zhang X, Olumi AF. 2007. MG-132 sensitizes TRAIL-resistant prostate cancer cells by activating c-Fos/c-Jun heterodimers and repressing c-FLIP(L). Cancer Res 67:2247–2255.

Liu J, Mao W, Ding B, Liang CS. 2008. ERKs/p53 signal transduction pathway is involved in doxorubicin-induced apoptosis in H9c2cells and cardiomyocytes. Am J Physiol Heart Circ Physiol 295:H1956–H1965.

Marshall C. 1999. How do small GTPase signal transduction pathways regulate cell cycle entry? Curr Opin Cell Biol 11:732–736.

Plotkin LI, Mathov I, Aguirre JI, Parfitt AM, Manolagas SC, Bellido T. 2005. Mechanical stimulation prevents osteocyte apoptosis: Requirement of integrins, Src kinases, and ERKs. Am J Physiol Cell Physiol 289:C633–C643.

Regula KM, Kirshenbaum LA. 2005. Apoptosis of ventricular myocytes: A means to an end. J Mol Cell Cardiol 38:3–13.

Rytomaa M, Lehmann K, Downward J. 2000. Matrix detachment induces caspase-dependent cytochrome *c* release from mitochondria: Inhibition by PKB/Akt but not Raf signalling. Oncogene 19:4461–4468.

Shen SC, Ko CH, Hsu KC, Chen YC. 2004. 3-OH flavone inhibition of epidermal growth factor-induced proliferaton through blocking prostaglandin E2 production. Int J Cancer 108:502–510.

Su B, Karin M. 1996. Mitogen-activated protein kinase cascades and regulation of gene expression. Curr Opin Immunol 8:402–411.

Sun B, Qi N, Shang T, Wu H, Deng T, Han D. 2010. Sertoli cell-initiated testicular innate immune response through toll-like receptor-3 activation is negatively regulated by Tyro3, Axl, and mer receptors. Endocrinology 151:2886–2897.

Suomela JP, Ahotupa M, Yang B, Vasankari T, Kallio H. 2006. Absorption of flavonols derived from sea buckthorn (Hippophae rhamnoides L.) and their effect on emerging risk factors for cardiovascular disease in humans. J Agric Food Chem 54:7364–7369.

Tantini B, Pignatti C, Fattori M, Fiumana E, Facchini A, Stefanelli C, Caldarera CM, Pegg AE, Flamigni F. 2004. Polyamine depletion inhibits etoposide-induced NF-kappaB activation in transformed mouse fibroblasts. Amino Acids 27:207–214.

Townsend KJ, Trusty JL, Traupman MA, Eastman A, Craig RW. 1998. Expression of the antiapoptotic MCL1 gene product is regulated by a mitogen activated protein kinase-mediated pathway triggered through microtubule disruption and protein kinase C. Oncogene 17:1223–1234.

Tran SE, Holmstrom TH, Ahonen M, Kahari VM, Eriksson JE. 2001. MAPK/ERK overrides the apoptotic signaling from Fas, TNF, and TRAIL receptors. J Biol Chem 276:16484–16490.

van Acker SA, Boven E, Kuiper K, van den Berg DJ, Grimbergen JA, Kramer K, Bast A, van der Vijgh WJ. 1997. Monohydroxyethylrutoside, a dose-dependent cardioprotective agent, does not affect the antitumor activity of doxorubicin. Clin Cancer Res 3:1747–1754.

von Harsdorf R, Li PF, Dietz R. 1999. Signaling pathways in reactive oxygen species-induced cardiomyocyte apoptosis. Circulation 99:2934–2941.

Ward NE, Gravitt KR, O'Brian CA. 1995. Irreversible inactivation of protein kinase C by a peptide-substrate analog. J Biol Chem 270:8056–8060.

Whitmarsh AJ, Davis RJ. 1996. Transcription factor AP-1 regulation by mitogen-activated protein kinase signal transduction pathways. J Mol Med (Berl) 74:589–607.

Xiao J, Sun B, Cai GP. 2010a. Transient expression of interferon-inducible p204 in the early stage is required for adipogenesis in 3T3-L1cells. Endocrinology 151:3141–3153.

Xiao J, Wang NL, Sun B, Cai GP. 2010b. Estrogen receptor mediates the effects of pseudoprotodiocsin on adipogenesis in 3T3-L1cells. Am J Physiol Cell Physiol 299:C128–C138.

Yamaji-Hasegawa A, Tsujimoto M. 2006. Asymmetric distribution of phospholipids in biomembranes. Biol Pharm Bull 29:1547–1553.

Youle RJ, Strasser A. 2008. The BCL-2 protein family: Opposing activities that mediate cell death. Nat Rev Mol Cell Biol 9:47–59.

Zhang N, Pei F, Wei H, Zhang T, Yang C, Ma G. 2009. Isorhamnetin protects rat ventricular myocytes from ischemia and reperfusion injury. Exp Toxicol Pathol 63:33–38.

Zhou B, Wang ZX, Zhao Y, Brautigan DL, Zhang ZY. 2002. The specificity of extracellular signal-regulated kinase 2 dephosphorylation by protein phosphatases. J Biol Chem 277:31818–31825.